Nuclear Instruments and Methods in Physics Research A 785 (2015) 9–13

Contents lists available at ScienceDirect

Nuclear Instruments and Methods in Physics Research A

journal homepage: www.elsevier.com/locate/nima

Detection of diamonds in kimberlite by the tagged neutron method

V.Yu. Alexakhin [a], V.M. Bystritsky [a], N.I. Zamyatin [a], E.V. Zubarev [a], A.V. Krasnoperov [a], V.L. Rapatsky [a], Yu.N. Rogov [a,*], A.B. Sadovsky [a], A.V. Salamatin [a], R.A. Salmin [a], M.G. Sapozhnikov [a], V.M. Slepnev [a], S.V. Khabarov [a], E.A. Razinkov [b], O.G. Tarasov [b], G.M. Nikitin [c]

[a] Neutron Technologies LLC, Dubna, Joint Institute for Nuclear Research, Dubna, Russia
[b] Neutron Technologies LLC, Dubna, Russia
[c] Institute "Yakutniproalmaz", ALROSA JSC, Mirny, Russia

ARTICLE INFO

Article history:
Received 22 December 2014
Received in revised form
17 February 2015
Accepted 23 February 2015
Available online 3 March 2015

Keywords:
Fast tagged neutrons
Diamonds
Kimberlite

ABSTRACT

A new technology for diamond detection in kimberlite based on the tagged neutron method is proposed. The results of experimental researches on irradiation of kimberlite samples with 14.1-MeV tagged neutrons are discussed. The source of the tagged neutron flux is a portable neutron generator with a built-in 64-pixel silicon alpha-detector with double-sided stripped readout. Characteristic gamma rays resulting from inelastic neutron scattering on nuclei of elements included in the composition of kimberlite are registered by six gamma-detectors based on BGO crystals. The criterion for diamond presence in kimberlite is an increased carbon concentration within a certain volume of the kimberlite sample.

1. Introduction

At present kimberlite ore is processed in crushers or grinding rolls with subsequent grinding in wet mills down to a size of 0.2 mm [1]. The basic disadvantage of the standard diamond processing technology is that crushing kimberlite ore can break the most valuable large diamonds of few carats.

We propose a new procedure for non-destructive detection of large-sized diamonds in kimberlite. The main idea of the proposed method is the irradiation of large kimberlite pieces with fast neutrons with an energy of 14 MeV produced in the nuclear reaction

$$d + {}^3H \rightarrow {}^4He + n. \quad (1)$$

Direction of a neutron is determined by detecting (tagging) the α-particle that accompanies the neutron using a special α-detector. Interacting with kimberlite, tagged neutrons induce inelastic scattering reactions

$$n + A \rightarrow n` + A^*, A^* \rightarrow \gamma + A. \quad (2)$$

During de-excitation of nuclei A* γ-rays are emitted with an energy spectrum specific for each chemical element present in the kimberlite. Characteristic γ-rays are registered by γ-detectors in coincidence with the signal from the α-detector. Measurement of the time interval between the signals from the α- and γ-detectors allows determining the distance from the neutron source to the point from which the γ-quantum is emitted since the neutron speed is constant and equals 5 cm/ns. Thus the tagged neutron method makes it possible to determine all three spatial coordinates of the examined sample volume.

The tagged neutron method (also called the Associated Particle Imaging (API) method) has been widely used [2–9] for constructing explosives and drug detectors, which allow determining elemental composition of the substance hidden in the examined objects of various sizes from hand luggage to shipping containers.

The search for diamonds by the tagged neutron method is reduced to detection of excess carbon at a particular point of the kimberlite sample. Large penetrability of fast neutrons makes it possible to examine appreciably large samples of kimberlite. Thus, rock pieces containing large-size diamonds can be identified before the crushing stage.

We developed a method for automatic detection of diamonds in kimberlite and created an experimental diamond detection setup, which we used to carry out experiments on estimation of detectable diamond size for various background conditions.

2. Description of the setup

The experimental setup for diamond detection in kimberlite consists of a portable neutron generator ING-27 with a built-in

* Corresponding author.
E-mail address: Yury.Rogov@cern.ch (Yu.N. Rogov).

http://dx.doi.org/10.1016/j.nima.2015.02.049
0168-9002/

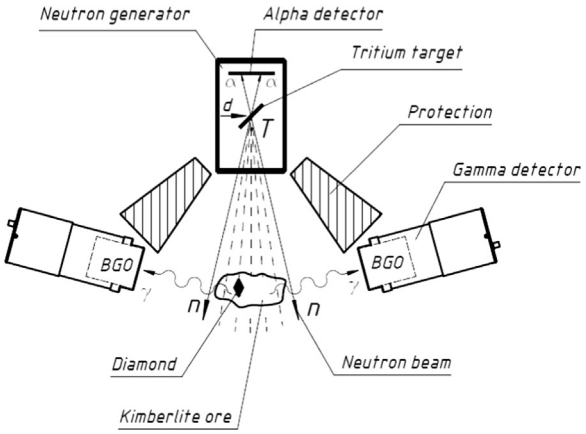

Fig. 1. General view of the experimental setup (top view).

64-pixel alpha-detector, six gamma-detectors based on BGO crystals, electronics of the data acquisition system for the alpha- and gamma-detectors, and power supply units for the neutron generator and the alpha- and gamma-detectors. The scheme of the setup is shown in Fig. 1.

The diamond simulant, made from pressed diamond sand, is attached to a set of suspension wires, which can also hold several kimberlite samples. The diamond simulant is typically located behind the kimberlite sample or between two samples of kimberlite.

2.1. Neutron generator

The ING-27 neutron generator is produced by the Dukhov All-Russian Research Institute of Automatics, Moscow. It operates in the DC mode with the maximal intensity $I=7\cdot 10^7$ s^{-1}. The size of the generator is 130 mm × 279 mm × 227 mm, and the weight is 8 kg.

The ING-27 neutron generator is usually equipped with a 9-channel alpha-detector. A unique 64-pixel silicon alpha-detector has been specially developed for diamond detection.

The 64-pixel silicon α-detector built into the neutron generator is a double-sided stripped detector that consists of eight mutually perpendicular strips on each side forming an 8×8 matrix of 4×4 mm^2 elements. The total sensitive area of the 64-element α-detector is 32×32 mm^2. The alpha-detector is located 62 mm away from the tritium target of the ING-27. The front-end electronics unit of the alpha-detector consists of 16 independent signal preamplifiers fed from 16 strips of the alpha-detector. The signal preamplifiers of the alpha-detector are mounted in the rear part of the neutron generator.

Spatial characteristics of 64 tagged neutron beams were measured by a scintillation stripped profilometer. Fig. 2 shows the spatial distribution of the tagged beams produced by the coincidences of the pulses from eight vertical strips with a single horizontal strip.

The width of each tagged beam is $\Gamma_X=(14.6\pm 0.9)$ mm and $\Gamma_Y=(14.8\pm 1.1)$ mm at a distance of 300 mm from the NG. This is consistent with the value expected from a pointlike deuteron beam hitting the target.

2.2. Gamma-detector

Six gamma-detectors based on BGO crystals with a diameter of 76 mm and thickness of 65 mm were used to detect gamma rays from the irradiated object.

These detectors have the following features:

– Energy resolution is (8–2.5) % within the energy range of 1–12 MeV. For the carbon gamma line ($E_\gamma=4.44$ MeV) the energy resolution of the gamma-detector is on average $\Gamma_E=(4.4\pm 0.1)$ %.
– High efficiency of gamma rays detection within the specified energy range.
– Low sensitivity for detection of background neutrons.

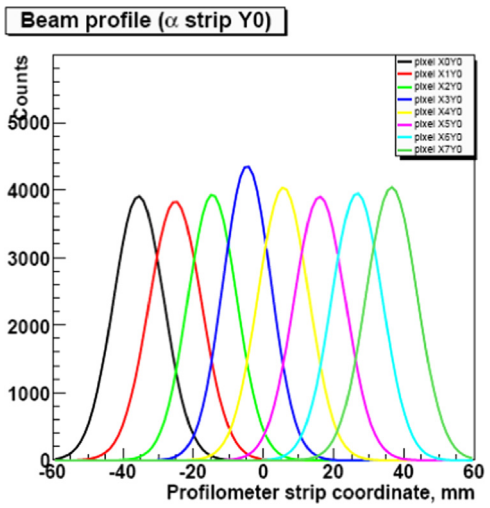

Fig. 2. Spatial distribution of eight tagged beams.

The time resolution of the (α–γ)-coincidence system averaged over the whole set of the gamma-detectors is $\Gamma_t=(3.1\pm 0.1)$ ns.

2.3. Data acquisition system

The recording electronics of the data acquisition system for the alpha- and gamma-detectors is designed as a single board with 32 inputs, which has the size of a standard PCI card and can be inserted in a PCI-E slot of a personal computer. The hardware data acquisition board utilizes high-speed ADC for sampling of input signals. The system of registration process signal from alpha- and gamma-detectors is based on the principle of waveform-digitizing with subsequent calculation of their time and amplitude characteristics.

Channels of digitizing signals from the detectors are built on the same scheme, which includes an amplifier with 0–20 MHz bandpass filter and ADC measurement interval of 10 ns (100 MHz). The digital code corresponding to each of measurement is fed to ADC programmable logic circuit, in which there is definition of moments of (α–γ)-coincidence in digital form.

Programmable scheme logic of the electronics board of DAQ system organizes the reception of information from the ADC, allocates of coincidence moment definition, prepares a data buffer and provides its transfer to PC memory. Subsequently the exact value of the pulse amplitudes and the time interval between them are calculated.

The special software for selection and signal processing extracts information about (α–γ)-coincidence, determines triggered channel numbers, calculates a time interval between pulses and the area under the pulse envelope, defining thereby an amount proportional to the energy released in the detectors, and counts the pulses detected by each detector individually. These parameters are presented in real-time histograms and stored in the data file.

3. Examined samples

For this investigation ALROSA JSC supplied us with diamond simulants, kimberlite and core samples from wells. At the first

stage we received 5 diamond simulants made of diamond powder, 6 kimberlite samples, and 3 core samples. The diamond simulants ranged in weight from 0.3 to 11.2 g and in overall dimensions from 5 to 20 mm. The linear dimensions of the kimberlite stones were of 8–15 cm with the corresponding widths of 2–4 cm. The core samples were cylinders 10 cm in diameter and 20 cm in length.

At the second stage of the investigation we were provided with 55 kg of kimberlite from the "Mir" mine. These kimberlite samples were 33 rocks of irregular shape with typical linear dimensions 10–20 cm and thickness of 4–10 cm.

4. Measurement procedure

Since diamonds entirely consist of carbon, the procedure of their detection consists in detecting excess carbon in any area of the kimberlite sample. The characteristic energy spectrum of gamma rays from a carbon sample is shown in Fig. 3.

As Fig. 3 shows, the 4.44-MeV gamma line uniquely points to the presence of carbon. Moreover, a single escape peak corresponding to the energy of 3.93 MeV is clearly observed. This simple shape of the carbon gamma-spectrum significantly simplifies carbon detection in kimberlite.

The energy spectrum of the gamma rays from the kimberlite is shown in Fig. 4 (dashed line). Oxygen lines at 6.13 MeV and 3.8 MeV are clearly observed. At the same time there is no carbon peak at 4.44 MeV. This also simplifies diamond identification.

To simulate the spectrum of diamond-bearing kimberlite, we attached a graphite cube of 25 mm to the kimberlite sample. The spectrum from this assembly is shown in Fig. 4 (solid line).

One can clearly see that the presence of carbon results in a peak at 4.44 MeV, which is absent in pure kimberlite (Fig. 4, dashed line).

A typical diamond simulant test is irradiation of the kimberlite+simulant assembly. The assembly is placed at a distance of 14 cm from the neutron generator, and the distance from the assembly to the gamma detectors is 30 cm. The neutron generator intensity is $I=5\times10^7\ s^{-1}$. The standard data-taking time is 30 min. We would like to emphasize that this time was chosen only for obtaining larger statistics to check the diamond detection procedure.

5. Measurement results

We irradiated 39 samples of the kimberlite ore. During the analysis each sample was divided into 64 regions in the plane perpendicular to the neutron beam direction. Only events within the energy range of 4.2–4.6 MeV corresponding to the carbon line were chosen. In each cell i, a value $\Sigma_i=(N-N_i)/\sigma_i$ was calculated, where N is the average number of events in the area of the carbon peak for the whole specimen, N_i is the number of events in the carbon peak region for this cell, and σ_i is the corresponding statistical error.

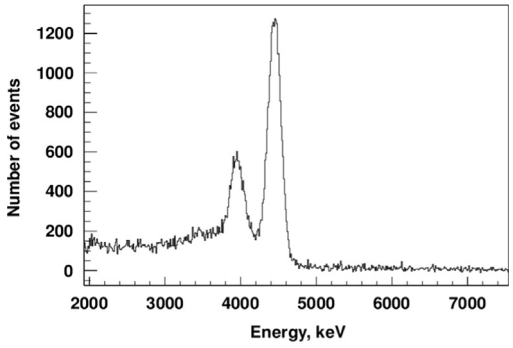

Fig. 3. Energy spectrum of gamma quanta for graphite (carbon).

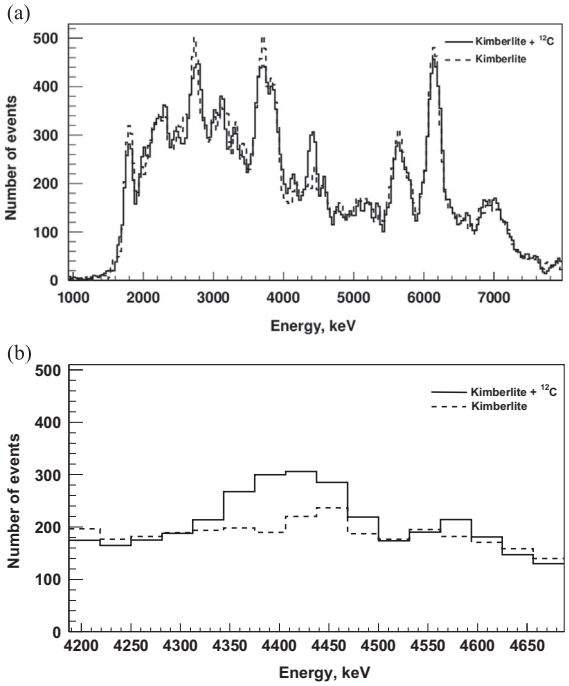

Fig. 4. Energy spectrum of gamma quanta from a kimberlite sample (solid line) and from a kimberlite+graphite cube assembly (dashed line) (a). Zoom of the region of the carbon peak (b).

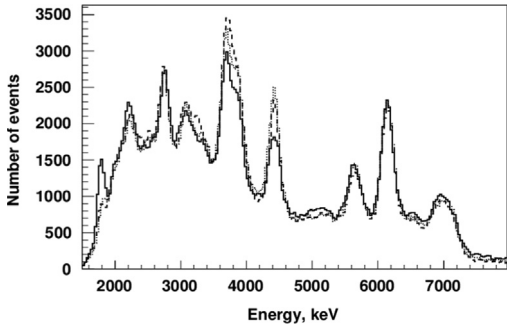

Fig. 5. Energy spectra of gamma quanta for 3 core samples (shown in different line styles).

It was found that for all samples the deviations from the average were no larger than 3σ. This is what is precisely expected for a homogeneous sample, where deviations of the carbon content from the average value are only due to statistical fluctuations.

The results for three core samples also exhibit no Σ_i fluctuations larger than 3. That is notable since the energy spectra of the core samples indicate a clear signal from the carbon fraction as shown in Fig. 5. Fig. 5 distinctly shows the carbon peak at 4.44 MeV. However, carbon presence in the elemental composition of the core sample did not result in a change in the *local* carbon concentration.

Fig. 6 shows the results of processing the data on irradiation of an assembly of a 2-cm-thick kimberlite stone and diamond simulants with different masses. The mass and diameter of the simulants are 11.2 g and 20 mm (Fig. 6a), 5.2 g and 15 mm (Fig. 6b), 1.78 g and 10 mm (Fig 6c), and 1.15 g and 8 mm (Fig. 6d). Cells with $0<\Sigma_i<3$ are shown filled with stars; cells with negative values of Σ_i are hatched. Cells with $\Sigma_i>3$ are shown in gray with designation of the value of the corresponding Σ_i.

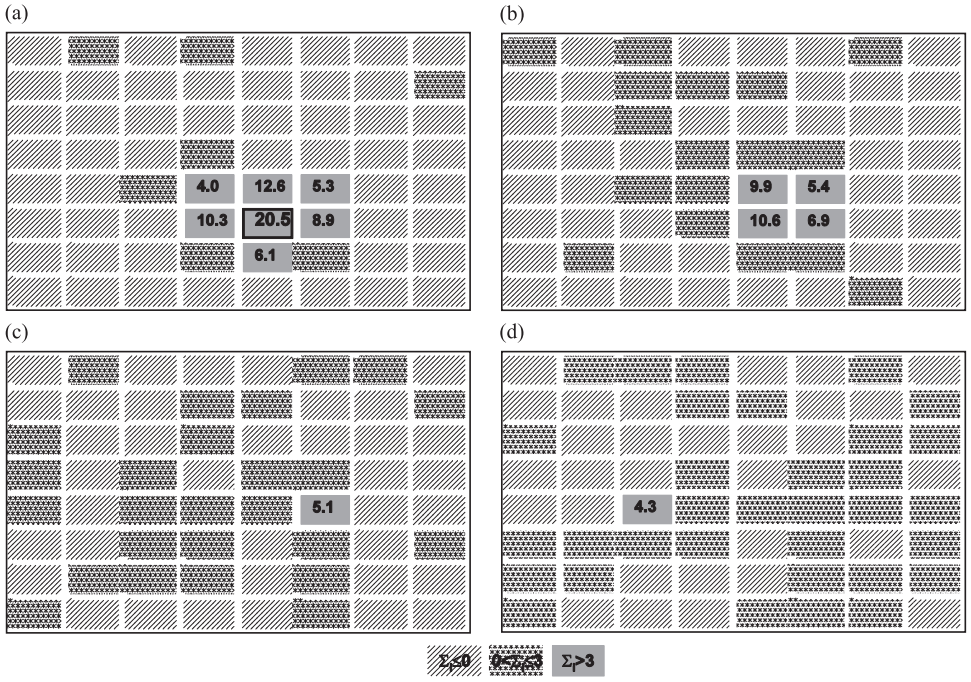

Fig. 6. Distribution of $\Sigma_i=(N-N_i)/\sigma$, where σ is the statistical error, for the kimberlite sample with the diamond imitators inside. The mass and diameter of the simulants are 11.2 g and 20 mm (a), 5.2 g and 15 mm (b), 1.78 g and 10 mm (c), and 1.15 g and 8 mm (d). Cells with $0<\Sigma_i<3$ are shown filled with stars, cells with negative values of Σ_i are hatched. Cells with $\Sigma_i>3$ are shown in gray with designation of the value of the corresponding Σ_i.

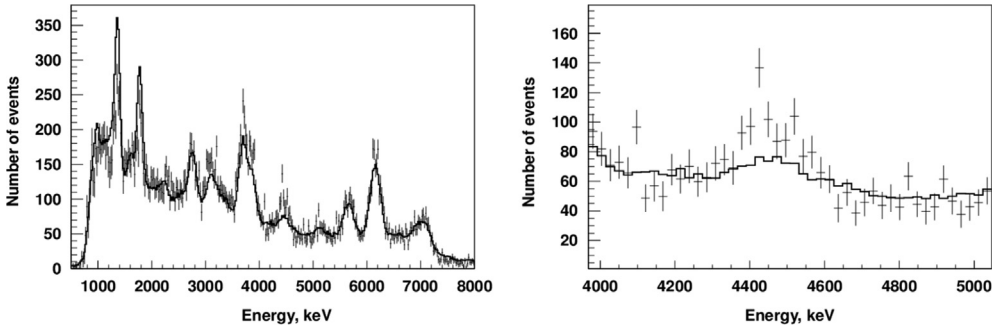

Fig. 7. Energy spectrum of the gamma-rays from kimberlite sample No. 17 (dots with error bars). The black solid line corresponds to the average spectrum of the gamma-rays from the other kimberlite samples (left). The region of the spectrum around the carbon line of 4.44 MeV is shown on the right plot.

For the large simulant of 11.2 g the carbon excess signal is seen in several cells (Fig. 6a). The excess of the recorded number of events in the carbon line above the average number of events for the sample is as large as 20.5σ. Thus, the signal is very sharp and distinct. It smoothly decreases with mass of the simulant. For the smallest simulant mass of 1.15 g it is shown in one cell (Fig. 6d) with the carbon excess value of $\Sigma_i=4.3$.

It is important that the spatial position of the diamond simulant in the kimberlite stone is correctly reproduced.

Upon completion of the first operation stage ALROSA supplied us with 33 kimberlite samples with a total weight 55 kg. The samples had a typical linear size of 15–20 cm and a weight of 1–2 kg.

When examining these kimberlite samples using the abovementioned procedure, we did not find any statistically significant excess of the local carbon content above the average value in 32 out of 33 stones. The observed deviation from the average value in all samples was no larger than 2.5σ. This indicates that the proposed procedure is characterized by a small false positive alarm rate (although statistics for confirmation of this statement is not sufficient yet).

In one of the samples (No. 17) a significant local carbon content excess above the average is detected. It ranges from 3.3 to 5.8σ depending on the angle at which the sample is irradiated. Fig. 7 shows the energy spectrum of the gamma-rays from kimberlite sample No. 17 (dots with error bars). The black solid line corresponds to the average spectrum of the gamma-rays from the other kimberlite samples (left). The region of the spectrum around the carbon line of 4.44 MeV is shown on the right plot.

After the samples returned to ALROSA JSC, sample No. 17 with excess carbon was analyzed there. Two inhomogeneous diamond inclusions with diameter up to 7 mm consisting of small diamond crystals with size from 1 to 2 mm were discovered. The photograph of the diamond inclusions is shown in Fig. 8.

Thus, the ability of the tagged neutron method to detect diamonds in kimberlite was experimentally proved. Of course, this experiment should be regarded as proof-of-principle one. The concrete characteristics of the neutron generator lifetime, time of measurements, rate of analysis of the kimberlite ore must be improved for the practical applications of the proposed method.

6. Discussions of the results

The finding of real diamonds is important to demonstrate the applicability of the tagged method which was not obvious from

Fig. 8. Two diamond inclusions found in kimberlite sample No. 17.

Table 1
Characteristics of different alpha detectors.

Type of neutron generator	Number of tagged beams	Size of the pixel (mm)	Spacing between pixels (mm)
ING-27 [7]	9	10	0.1
Sodern, Euritrack [10]	64	5.8	0.2
API-120 [11]	256	3	–
Present work	64	4	–

the beginning. The time resolution of the (α–γ)-coincidence system is quite large $\Gamma_t=(3.1\pm0.1)$ ns. It means that the spatial resolution in the direction of the neutron momentum is about 15 cm. The typical dimension of a diamond is few millimeters and it was absolutely not clear that in the specific region of the carbon line of 4.44 MeV its signal could dominate the signal from the background substance. Two features help to overcome the problem.

One is the high granularity of the alpha-detector. To our knowledge, the 4-mm-wide cell of the alpha-detector is one of the best results for the API technique. Characteristics of different alpha-detectors are compared in Table 1. Second, is the point-like deuteron beam of the ING-27. These features provide small spatial resolution in the plane perpendicular to the neutron momentum.

The large number of strongly intersected tagged beams (see, Fig. 2) helps in case of a diamond situated on the boundary of two tagged beams.

7. Conclusions

The technology for diamond detection in kimberlite based on the tagged neutron method is developed. An experimental setup based on a portable neutron generator with a built-in 64-pixel silicone alpha-detector is created. The energy spectrum of the gamma-rays from kimberlite is measured by 6 BGO gamma-detectors. Diamonds are identified by detecting a local carbon excess in the examined sample.

Measurements with 6 kimberlite and 3 core samples do not show any local excess of the number of events above the average in the carbon line region, whereas measurements with a combination of diamond simulants and kimberlite samples of different size and weight show the local excess of the number of events around 4.44 MeV. The minimal detectable mass of a diamond simulant is 1.15 g with a 1-cm-thick screening kimberlite layer in front of the simulant.

The subsequent check of the identification algorithm on 33 kimberlite samples with a total weight of 55 kg confirmed the potential of the tagged neutron method: false alarms were not detected, and the sample with a local carbon content excess from 3.3 to 5.8σ was found to have two inhomogeneous diamond inclusions up to 7 mm in diameter consisting of small diamonds with a size of 1 to 2 mm.

Acknowledgments

The authors are grateful to E.P. Bogolyubov, Yu.K. Presnyakov, V.I. Ryzhkov, T.O. Khasayev, A.S. Chuprikov, and D.I. Yurkov from Dukhov All-Russian Research Institute of Automatics for creation of the neutron generator with unique parameters, and to A.S. Chaadaev and O.E. Kovalchuk (ALROSA JSC) for very helpful comments.

References

[1] M.V. Verkhoturov, S.A. Amelin, N.I.R. Konnova, Diamonds Enrichment, Krasnoyarsk, 2009,207.
[2] P.O. Hawkins, R.W. Sutton, Review of Scientific Instruments 31 (1960) 241.
[3] L.I. Ussery, et al., Los Alamos National Lab report LA12847-MS (1994).
[4] E. Rhodes, et al., SPIE 2092 (1993) 288;
E. Rodes, et al., IEEE Transactions on Nuclear Science NS39 (1992) 1041.
[5] A. Beyerle, J.P. Hurley, L. Tunnell, Nuclear Instruments and Methods A299 (1990) 458.
[6] S. Pesente, et al., Nuclear Instruments and Methods A531 (2004) 657.
[7] V.M. Bystritsky, et al., Physics of Particles and Nuclei Letters 5 (2008) 441.
[8] V.M. Bystritsky, et al., Physics of Particles and Nuclei Letters 5 (2013) 722.
[9] V. Valkovic, et al., Nuclear Instruments and Methods A703 (2013) 133.
[10] S. Pesente, et al., Nuclear Instruments and Methods B261 (2007) 268.
[11] J. Michalzo, et al., Proceedings of the International Conference "Portable neutron generators and technologies on their basis", All-Russia Research Institute of Automatics-VNIIA, (Eds.: Barmakov, Yu.N.), Moscow, 2012, p.198–212.